J Mol Model (2010) 16:291–302
DOI 10.1007/s00894-009-0552-8

ORIGINAL PAPER

An experimental and theoretical approach to the molecular structure of 2-{4-[3-(2,5-dimethylphenyl)-3-methylcyclobutyl]thiazol-2-yl}isoindoline-1,3-dione

Namık Özdemir · Muharrem Dinçer · Alaaddin Çukurovalı

Received: 6 May 2009 / Accepted: 9 June 2009 / Published online: 12 July 2009

Abstract The title compound, 2-{4-[3-(2,5-dimethylphenyl)-3-methylcyclobutyl]thiazol-2-yl}isoindoline-1,3-dione ($C_{24}H_{22}N_2O_2S$), was synthesized and characterized by IR-NMR spectroscopy and single-crystal X-ray diffraction. The compound crystallizes in the monoclinic space group $P2_1/c$ with a=19.7799(13) Å, b=6.7473(4) Å, c=15.7259(9) Å and β=103.416(5)°. In addition, the molecular geometry, vibrational frequencies and gauge including atomic orbital (GIAO) ^{1}H and ^{13}C chemical shift values of the title compound in the ground state have been calculated by using the Hartree-Fock (HF) and density functional method (DFT/B3LYP) with 6–31G(d), 6–31 + G(d,p) and LANL2DZ basis sets, and compared with the experimental data. To determine conformational flexibility, molecular energy profile of the title compound was obtained by semi-empirical (AM1) calculations with respect to two selected degrees of torsional freedom, which were varied from −180° to +180° in steps of 5°. Besides, molecular electrostatic potential, frontier molecular orbitals (FMO) analysis and thermodynamic properties of the title compound were investigated by theoretical calculations.

Keywords AM1 semi-empirical method · Conformational analysis · DFT · Frontier molecular orbitals · GIAO · HF · IR and NMR spectroscopy · Molecular electrostatic potential · Vibrational assignment · X-ray structure determination

Introduction

The chemistry of aminothiazoles and their derivatives has attracted the attention of chemists, since they exhibit important biological activity in medicinal chemistry [1], such as antibiotic, anti-inflammatory, antihelmintic or fungicidal properties [2–4]. 2-Aminothiazoles are known mainly as biologically active compounds with a broad range of activities and as an intermediates in the synthesis of antibiotics, well known sulfa drugs, and some dyes [5, 6]. It has been shown that 3-substituted cyclobutane carboxylic acid derivatives have antidepressant activities and liquid crystal properties [7]. At the same time, it has been found that some isoindole-1,3-dione derivatives have protein kinase CK2 (Casein Kinase 2) activity [8].

Recent papers in the literature concerning the calculation of NMR chemical shift (c.s.) by quantum-chemistry methods display that geometry optimization is a crucial factor in an accurate determination of computed NMR chemical shift [9–12]. The gauge-including atomic orbital (GIAO) [13, 14] method is one of the most common approaches for calculating nuclear magnetic shielding tensors. It has been shown to provide results that are often more accurate than those calculated with other approaches, at the same basis set

Electronic supplementary material The online version of this article (doi:10.1007/s00894-009-0552-8) contains supplementary material, which is available to authorised users.

N. Özdemir (✉) · M. Dinçer
Department of Physics,
Faculty of Arts and Sciences,
Ondokuz Mayıs University,
55139 Kurupelit, Samsun, Turkey
e-mail: namiko@omu.edu.tr

A. Çukurovalı
Department of Chemistry,
Faculty of Arts and Sciences,
Fırat University,
23119 Elazığ, Turkey

size [15]. In most cases, in order to take into account correlation effects, post-Hartree-Fock calculations of organic molecules have been performed using (i) Møller-Plesset perturbation methods, which are very time consuming and hence applicable only to small molecular systems, and (ii) density functional theory (DFT) methods, which usually provide significant results at a relatively low computational cost [16]. In this regard, DFT methods have been preferred in the study of large organic molecules [17], metal complexes [18] and organometallic compounds [19] and for GIAO ^{13}C c.s. calculations [15] in all those cases in which the electron correlation contributions were not negligible.

In this study, the geometrical parameters, fundamental frequencies and GIAO ^{1}H- and ^{13}C-NMR chemical shifts of the title compound in the ground state have been calculated by using the HF and DFT (B3LYP) methods with 6-31G(d), 6-31 + G(d,p) and LANL2DZ basis sets. A comparison of the experimental and theoretical spectra can be very useful in making correct assignments and understanding the basic chemical shift-molecular structure relationship. And so, these calculations are valuable for providing insight into molecular analysis.

Experimental

Synthesis

All chemicals were of reagent grade and used as commercially purchased without further purification. IR spectra of the compound were recorded in the range of 400–4000 cm^{-1} with a Mattson 1000 FT-IR spectrometer using KBr pellets. The ^{1}H- and ^{13}C-NMR spectra were recorded on a Varian-Mercury 400 MHz spectrometer. Melting point was determined by Gallenkamp melting point apparatus and is uncorrected. The synthesis of the title compound was simply carried out in the following reaction scheme (Fig. 1). A mixture of 1.4812 gr (10 mmol) of phthalanhydride and 2.7241 g (10 mmol) of 4-[3-(2,5-dimethyl-phenyl)-3-methyl-cyclobutyl]-thiazol-ylamine was heated slightly over the melting point of the mixture of two starting materials, desired compound was formed immediately as bulky powder. The shiny crystals, which are suitable for X-ray analysis, were obtained by the crystallization from ethanol (yield: 95%; m.p. 421 K).

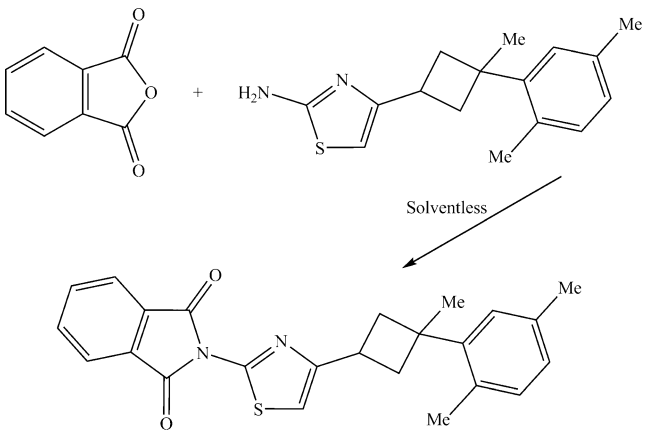

Fig. 1 Synthesis scheme of the title compound

Crystal data for the title compound

CCDC 712984, $C_{24}H_{22}N_2O_2S$, M_w=402.50, monoclinic, space group $P2_1/c$; Z=4, a=19.7799(13), b=6.7473(4), c=15.7259(9) Å, α=γ=90, β=103.416(5)º; V=2041.5(2) Å^3, $F(000)$=848, D_x=1.310 Mg/m^3. Full crystallographic data are available as supplementary material.

Computational details

The molecular structure of the title compound in the ground state (*in vacuo*) is optimized by HF and B3LYP methods with 6–31G(d), 6–31 + G(d,p) and LANL2DZ basis sets. Then vibrational frequencies for optimized molecular structures have been calculated. The vibrational frequencies for these species are scaled by 0.8929 and 0.9613, 0.89 and 0.96, 0.9393 and 0.9978, respectively. The geometry of the title compound, together with that of tetramethylsilane (TMS), is fully optimized. ^{1}H- and ^{13}C-NMR chemical shifts are calculated within GIAO approach [13, 14] applying B3LYP and HF method [20] with 6–31G(d) [21], 6–31 + G (d,p) [22] and LANL2DZ [23–25] basis sets. Generally, reliable predictions of optimized geometrical parameters, frequencies and chemical shifts require several elements: adequate basis sets, sufficient electron correlation effects. Besides, the choice of the basis set is also a critical point in any computational study on molecular properties. In order to investigate the basis set effect on result, we take into account three types of basis functions: (i) 6–31G(d) for checking polarization function effect, (ii) 6–31 + G(d,p) for checking both polarization function and diffuse effects, and (iii) LANL2DZ for checking some effective core potentials. The ^{1}H- and ^{13}C-NMR chemical shifts are converted to the TMS scale by subtracting the calculated absolute chemical shielding of TMS ($\delta = \Sigma_0 - \Sigma$, where δ is the chemical shift, Σ is the absolute shielding and Σ_0 is the absolute shielding of TMS), whose values are 32.52 and 199.79 ppm for HF/6–31G(d), 31.88 and 201.25 ppm for HF/6–31 + G(d,p), 33.19 and 203.36 ppm for HF/LANL2DZ, 32.10 and 189.40 ppm for B3LYP/6–31G(d), 31.56 and 192.41 ppm for B3LYP/6–31 + G(d,p), and 32.76 and 193.54 ppm for B3LYP/LANL2DZ, respectively. All the calculations are performed by using GaussView molecular visualization program [26] and Gaussian 03 program package [27] on

personal computer without specifying any symmetry for the title molecule. A preliminary search of low-energy structures has been carried out with the AM1 computations. Conformational energies were calculated as a one-dimensional scan by varying the φ_1(S1–C9–N1–C8) and φ_2(C13–C14–C17–C18) dihedral angles from −180° to +180° in steps of 5°, and the molecular energy profiles were obtained.

Results and discussion

Description of the crystal structure

The title compound, an Ortep-3 [28] view of which is shown in Fig. 2, crystallizes in the monoclinic space group $P2_1/c$ with four molecules in the unit cell. The asymmetric unit in the crystal structure contains only one molecule. The title molecule is composed of a central thiazole ring, with an isoindoline-1,3-dione group connected to the 2-position of the ring and a 1,4-dimethyl-2-(1-methylcyclobutyl) benzene group in the 4-position. The thiazole ring is planar with a maximum deviation of 0.0057(14) Å for atom C10. In the crystal structure, the 2,5-dimethylbenzene ring and 2-(thiazol-2-yl)isoindoline-1,3-dione group are in *cis* positions with respect to the cyclobutane ring. The dihedral angles between the thiazole plane *A* (S1/N2/C9-C11), the benzene plane *B* (C17-C22), the cyclobutane plane *C* (C12-C15) and the isoindoline plane *D* (O1/O2/N1/C1-C8) are 80.62(7)° (*A*/*B*), 81.17(10)° (*A*/*C*), 52.61(5)° (*A*/*D*), 30.04 (13)° (*B*/*C*), 64.25(6)° (*B*/*D*) and 88.65(9)° (*C*/*D*).

Although close to being planar, the cyclobutane ring is puckered. The C13/C14/C15 plane forms a dihedral angle of 28.84(22)° with the C15/C12/C13 plane. This value is significantly bigger than those in the literatures; 23.5 [29], 25.74(6) [30] and 19.26(17)° [31]. However, when the bond lengths and angles of the cylobutane ring in the title compound are compared with these, it is seen that there are no significant differences.

There are two obviously different C—N bond distances in the thiazole ring, *viz*. N2—C9 and N2—C11. The C10—C11 bond distance is 1.347(3) Å, characterizing a C=C double bond. The S1—C9 and S1—C10 bond lengths (Table 2) are shorter than the accepted value for an S—Csp^2 single bond (1.76 Å; [32]), resulting from the conjugation of the electrons of atom S1 with atoms C9 and C10. Since the interbond angles at three-connected C atoms and at two-connected N atoms are optimally ~120°, the constraints of a planar five-membered ring combined with the fact that the C—S bond distances are significantly longer than the other ring bonds lead to an interbond angle at S that is somewhat less than 90°, consistent with the use of only *p* orbitals by the S atom in the formation of the σ framework [33]. The two carboxyl C=O bonds are of the same length, being 1.204(3) Å. All three C—N bonds around N1 are coplanar, indicating trigonal hybridization of the ring nitrogen. The angle between the five- and six-membered rings of the isoindoline system is 1.70(8)°, and the maximum deviation from planarity is 0.0332(20) Å for atom C3.

In the molecular structure of the title compound, the interatomic distance between thiophene atom S1 and the carboxyl atom O2 is 3.193 Å, which is less than the sum of the atomic van der Waals radii for sulphur and oxygen, 1.80 and 1.52 Å, respectively [34]. This indicates that there are an attractive intramolecular interaction between S and O atoms, which is called σ-hole bonding [35–37]. In the

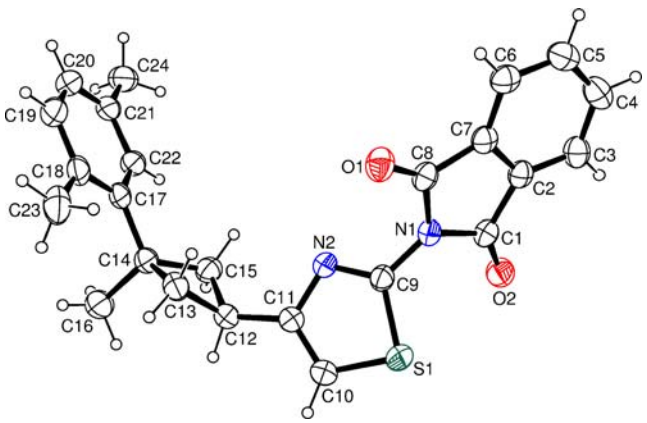

Fig. 2 A view of the title compound showing the atom-numbering scheme. Displacement ellipsoids are drawn at the 30% probability level and H atoms are shown as small spheres of arbitrary radii

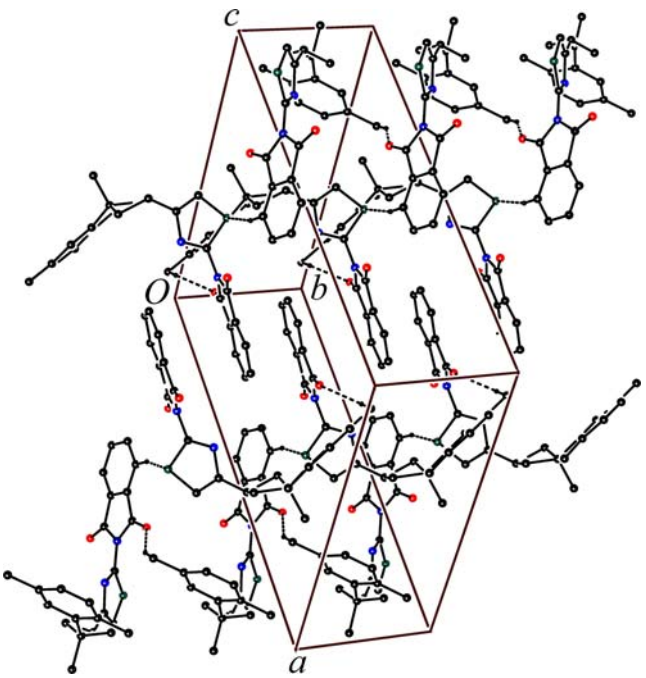

Fig. 3 Part of the crystal structure of the title compound, showing the C—H···S, C—H···O and π— π stacking interactions. For the sake of clarity, H atoms not involved in H-bonds have been omitted

Table 1 Hydrogen bonding geometry for the title compound

D—H···A	D—H (Å)	H···A (Å)	D···A (Å)	D—H···A (°)
C6—H6···S1^{i}	0.93	2.82	3.704(3)	160
C24—H24B···O1^{ii}	0.96	2.58	3.468(3)	155

Symmetry codes: (i) x,−y+3/2, z−1/2; (ii) x, y−1, *z*

crystal structure (Fig. 3 and Table 1), molecules of the title compound are packed in columns running along the *b* axis. The molecules in each column are linked to one another *via* C—H···O hydrogen bonds, in which methyl atom C24 in the molecule at (*x*, *y*, *z*) acts as hydrogen-bond donor, *via* atom H24B, to carboxyl atom O1 in the molecule at (*x*, *y*−1, *z*), resulting in the formation of molecular chains along the *b* axis. Besides, there are C—H···S interactions between the molecules in glide-related columns, in which aryl atom C6 in the molecule at (*x*, *y*, *z*) acts as hydrogen-bond donor, *via* atom H6, to thiophene atom S1 in the molecule at $(x, -y+3/2, z-1/2)$. Glide-related columns are connected to similar neighboring columns by means of π—π stacking interactions. In these interactions, the five- and six-membered rings of the isoindoline groups of the molecules at (*x*, *y*, *z*) and (1−*x*, 1−*y*, 1−*z*) are mutually parallel, with a distance of 3.655(5) Å between the ring centroids, and a perpendicular distance of 3.320(5) Å between the rings. There are no other significant intermolecular interactions in the crystal structure of the title compound.

Theoretical structures

Some selected geometric parameters experimentally obtained and theoretically calculated by HF and B3LYP methods with 6–31G(d), 6–31 + G(d,p) and LANL2DZ basis sets are listed in Table 2. When the X-ray structure of the title compound is compared with its optimized counterparts (see Fig. 4), conformational discrepancies are observed between them. The dihedral angles between *A, B, C* and *D* planes are calculated at 83.594° (*A*/*B*), 89.913° (*A*/*C*), 89.576° (*A*/*D*), 35.276° (*B*/*C*), 56.421° (*B*/*D*) and 89.016° (*C*/*D*) for HF/6–31G(d), at 83.237° (*A*/*B*), 89.899° (*A*/*C*), 89.844° (*A*/*D*), 35.356° (*B*/*C*), 55.901° (*B*/*D*) and 89.584° (*C*/*D*) for HF/6–31 + G(d,p), at 82.808° (*A*/*B*), 89.859° (*A*/*C*), 89.998° (*A*/*D*), 35.600° (*B*/*C*), 56.000° (*B*/*D*) and 89.378° (*C*/*D*) for HF/LANL2DZ, at 83.440° (*A*/*B*), 87.293° (*A*/*C*), 10.574° (*A*/*D*), 35.338° (*B*/*C*), 78.797° (*B*/*D*) and 85.978° (*C*/*D*) for B3LYP/6–31G(d), at 81.347° (*A*/*B*), 89.264° (*A*/*C*), 88.732° (*A*/*D*), 35.733° (*B*/*C*), 57.582° (*B*/*D*) and 88.067° (*C*/*D*) for B3LYP/6–31 + G(d,p), and at 79.789° (*A*/*B*), 88.730° (*A*/*C*), 85.834° (*A*/*D*), 35.672° (*B*/*C*), 59.282° (*B*/*D*) and 87.409° (*C*/*D*) for B3LYP/LANL2DZ. According to X-ray study, dihedral angle between the C13/C14/C15 and C15/C12/C13 planes is 28.84(22)°, whereas the dihedral angle has been calculated at 26.442° for HF/6–31G(d), at 26.393° for HF/6–31 + G(d,p), at 25.582° for HF/LANL2DZ, at 26.450° for B3LYP/6–31G(d), at 25.974° for B3LYP/6–31 + G(d,p), and at 25.700° for B3LYP/LANL2DZ.

Using the root mean square error (RMSE) for evaluation, HF/6–31 + G(d,p) is the *ab initio* calculation that best predicts the bond distances, with a value of 0.014 Å, whereas the B3LYP/LANL2DZ level is further off with an RMSE of 0.043 Å. The B3LYP/6–31 + G(d,p) calculation is those that provide the lowest RMSE for bond angles (0.870°). The highest RMSE's for bond angles are obtained at the LANL2DZ levels of calculations, with a value of 1.247° and 1.208° for the HF and B3LYP, respectively. A logical method for globally comparing the structures obtained with the theoretical calculations is by superimposing the molecular skeleton with that obtained from X-ray diffraction, giving an RMSE of 0.668 Å for HF/6–31G(d), 0.675 Å for HF/6–31 + G(d,p), 0.684 Å for HF/LANL2DZ, 0.527 Å for B3LYP/6–31G(d), 0.665 Å for B3LYP/6–31 + G(d,p) and 0.691 Å for B3LYP/LANL2DZ calculations (Fig. 4).

Conformational analysis

Based on HF/6–31G(d), HF/6–31 + G(d,p), HF/LANL2DZ, B3LYP/6–31G(d), B3LYP/6–31 + G(d,p) and B3LYP/LANL2DZ optimized geometries, the total energy of the title compound has been calculated by these methods, which are −1577.8034, −1577.8640, −1189.7831, −1585.9582, −1586.0280 and −1197.6535 a.u., respectively, while the dipole moment has been calculated as 2.6940, 2.6406, 2.7480, 3.2714, 2.2795 and 2.4219 Debye. In order to define the preferential position of the isoindoline fragment with respect to the thiazole ring, and the preferential position of the benzene ring with respect to the cyclobutane ring, respectively, a preliminary search of low energy structures was performed using AM1 computations as a function of the selected degrees of torsional freedom, φ_1(S1—C9—N1—C8) and φ_2(C13—C14—C17—C18). The respective values of the selected degrees of torsional freedom, φ_1(S1—C9—N1—C8) and φ_2(C13—C14—C17—C18), are −129.00(19) and −47.6(3)° in X-ray structure, whereas the corresponding values in optimized geometries are −94.64415 and −47.48217° for HF/6–31G(d), −94.95609 and −47.79393° for HF/6–31 + G(d,p), −92.71944 and −48.06459° for HF/

Table 2 Optimized and experimental geometric parameters of the title compound in the ground state

Parameters	X-ray	Calculated					
		HF			B3LYP		
		6–31G(d)	6–31 + G(d,p)	LANL2DZ	6–31G(d)	6–31 + G(d,p)	LANL2DZ
Bond lengths (Å)							
S1—C9	1.719(2)	1.727	1.724	1.788	1.769	1.749	1.827
S1—C10	1.694(2)	1.725	1.725	1.778	1.738	1.730	1.791
O1—C8	1.204(3)	1.183	1.184	1.212	1.204	1.211	1.238
O2—C1	1.204(2)	1.183	1.184	1.212	1.214	1.211	1.238
N1—C1	1.402(3)	1.401	1.400	1.412	1.417	1.422	1.436
N1—C8	1.423(3)	1.401	1.401	1.412	1.442	1.422	1.435
N1—C9	1.402(3)	1.405	1.407	1.404	1.401	1.407	1.409
N2—C9	1.290(3)	1.268	1.269	1.278	1.297	1.298	1.306
N2—C11	1.385(3)	1.382	1.382	1.404	1.383	1.381	1.405
C10—C11	1.347(3)	1.345	1.347	1.352	1.366	1.373	1.379
C11—C12	1.482(3)	1.497	1.497	1.494	1.496	1.497	1.498
C12—C13	1.532(3)	1.545	1.544	1.556	1.555	1.556	1.568
C12—C15	1.539(3)	1.545	1.545	1.556	1.556	1.556	1.568
C13—C14	1.545(3)	1.557	1.557	1.568	1.567	1.567	1.579
C14—C15	1.547(3)	1.556	1.556	1.568	1.565	1.566	1.577
C14—C16	1.536(3)	1.537	1.538	1.546	1.542	1.543	1.552
C14—C17	1.522(3)	1.525	1.526	1.527	1.524	1.525	1.530
RMSE[a]		0.015	0.014	0.030	0.021	0.018	0.043
Max. difference[a]		0.031	0.031	0.084	0.050	0.036	0.108
Bond angles (°)							
C9—S1—C10	88.61(11)	88.007	88.072	87.004	87.409	88.187	86.543
C1—N1—C8	111.29(18)	112.561	112.455	111.960	111.028	111.918	111.658
C1—N1—C9	123.90(18)	123.493	123.476	123.932	123.590	123.789	123.924
C8—N1—C9	124.77(18)	123.470	123.456	123.915	125.374	123.941	124.302
C9—N2—C11	110.00(18)	111.249	111.258	113.278	111.289	111.286	112.935
N1—C9—N2	124.01(19)	123.123	122.947	124.262	123.219	123.567	125.024
N2—C9—S1	115.59(16)	115.741	115.792	114.543	115.264	115.272	114.437
N1—C9—S1	120.38(16)	121.136	121.261	121.195	121.510	121.161	120.534
N2—C11—C12	120.24(19)	119.233	119.361	119.067	119.012	119.653	119.399
C11—C10—S1	111.29(18)	110.573	110.554	111.408	111.370	110.828	111.854
C10—C11—N2	114.5(2)	114.430	114.324	113.766	114.663	114.427	114.230
C10—C11—C12	125.3(2)	126.337	126.315	127.167	126.324	125.921	126.371
C11—C12—C13	118.9(2)	118.512	118.565	118.127	118.428	118.613	118.170
C11—C12—C15	120.42(19)	118.472	118.514	118.082	118.472	118.445	117.945
C13—C12—C15	87.37(17)	87.867	87.922	88.170	87.728	87.827	87.976
C12—C13—C14	89.40(18)	89.395	89.372	89.330	89.487	89.487	89.374
C17—C14—C16	108.37(18)	109.706	109.730	109.639	109.768	109.851	109.761
C17—C14—C13	121.1(2)	118.949	118.866	118.883	118.991	118.751	118.692
C16—C14—C13	111.6(2)	112.100	112.119	112.041	111.911	112.046	111.991
C17—C14—C15	116.8(2)	116.737	116.756	116.782	116.796	116.902	117.025
C16—C14—C15	110.8(2)	110.608	110.616	110.547	110.666	110.470	110.401
C13—C14—C15	86.65(17)	87.053	87.067	87.314	86.997	87.098	87.298
C12—C15—C14	89.10(18)	89.424	89.403	89.347	89.512	89.541	89.449
RMSE[a]		0.945	0.954	1.247	0.914	0.870	1.208

Table 2 (continued)

Parameters	X-ray	Calculated					
		HF			B3LYP		
		6–31G(d)	6–31 + G(d,p)	LANL2DZ	6–31G(d)	6–31 + G(d,p)	LANL2DZ
Max. difference[a]		2.151	2.234	3.278	2.109	2.349	2.935
Dihedral angles (°)							
C1—N1—C9—N2	−124.7(2)	−86.202	−85.346	−87.280	−170.512	−84.933	−83.285
C8—N1—C9—N2	52.7(3)	85.294	85.004	87.260	10.588	87.697	92.465
C1—N1—C9—S1	53.6(3)	93.860	94.694	92.741	10.500	94.789	95.851
C8—N1—C9—S1	−129.00(19)	−94.644	−94.956	−92.719	−168.401	−92.581	−88.399
N2—C11—C12—C13	−64.1(3)	−52.004	−52.046	−51.865	−48.694	−52.878	−53.260
C10—C11—C12—C15	−138.1(2)	−127.747	−127.646	−127.747	−124.161	−128.563	−129.441
C11—C12—C13—C14	144.2(2)	140.345	140.406	139.329	140.242	139.984	139.137
C11—C12—C15—C14	−142.8(2)	−140.389	−140.463	−139.378	−140.229	−140.155	−139.367
C13—C14—C17—C22	137.1(2)	135.557	135.208	134.927	134.557	133.804	132.866
C15—C14—C17—C18	−150.8(2)	−149.773	−150.063	−150.685	−150.674	−151.465	−152.926

[a] RMSE and maximum differences between the bond lengths and angles computed by the theoretical methods and those obtained from X-ray diffraction

LANL2DZ, −168.40105 and −48.38952° for B3LYP/6–31G(d), −92.58062 and −49.13034° for B3LYP/6–31 + G(d,p), and −88.39890 and −50.28458° for B3LYP/LANL2DZ. Molecular energy profiles with respect to rotations about the selected torsion angles are presented in Fig. 5. According to the results, the low energy domains for φ_1(S1—C9—N1—C8) are located at −100 and 105° having energy of −50.663 kcal mol^{-1}, while they are located at −45, and 145° having energy of −50.778 and 50.692 kcal mol^{-1}, respectively, for φ_2(C13—C14—C17—C18). Energy difference between the most favorable and unfavorable conformers, which arises from rotational potential barrier calculated with respect to the two selected torsion angles, is calculated as 2.020 kcal mol^{-1} for φ_1(S1—C9—N1—C8) and as 7.343 kcal mol^{-1} for φ_2(C13—C14—C17—C18), when both selected degrees of torsional freedom are considered.

Molecular electrostatic potential

The molecular electrostatic potential (MEP) was determined using B3LYP/6–31G(d) method. Molecular electrostatic potential is related to the electronic density and is a very useful descriptor in understanding sites for electrophilic attack and nucleophilic reactions as well as hydrogen bonding interactions [38–40]. The negative (red color) regions of MEP were related to electrophilic reactivity and the positive (blue color) ones to nucleophilic reactivity shown in Fig. 6. As can be seen in Fig. 6, there are two possible sites on the title compound for electrophilic attack. The negative regions are mainly localized on the carbonyl oxygen atoms, O1 and O2, with a maximum value of −0.067 a.u. However, the maximum positive regions are mainly over the C3—H3/C4—H4/C5—H5/C6—H6 bonds, which can be considered as possible sites for nucleophilic attack, with a maximum value

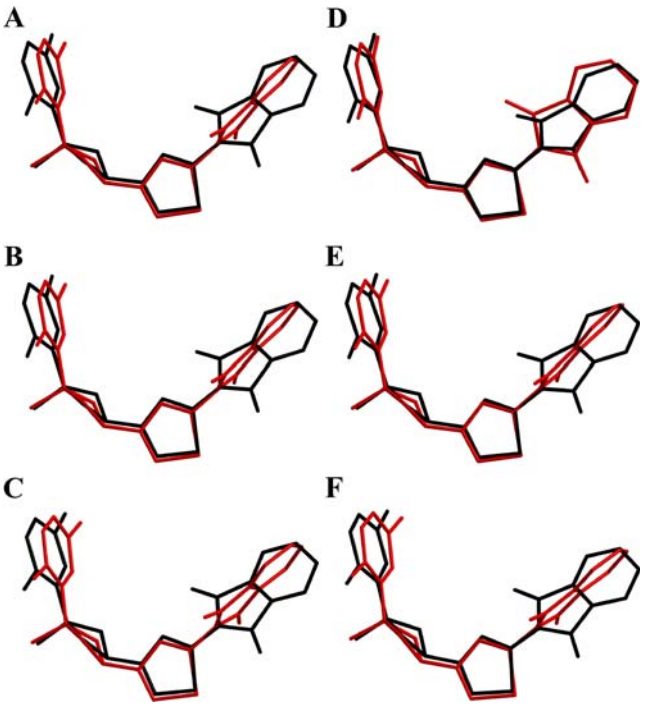

Fig. 4 Atom-by-atom superimposion of the structures calculated (red) [**A**=HF/6–31G(d), **B**=HF/6–31 + G(d,p), **C**=HF/LANL2DZ, **D**=B3LYP/6–31G(d), **E**=B3LYP/6–31 + G(d,p) and **F**=B3LYP/LANL2DZ] over the X-ray structure (black) for the title compound. Hydrogen atoms omitted for clarity

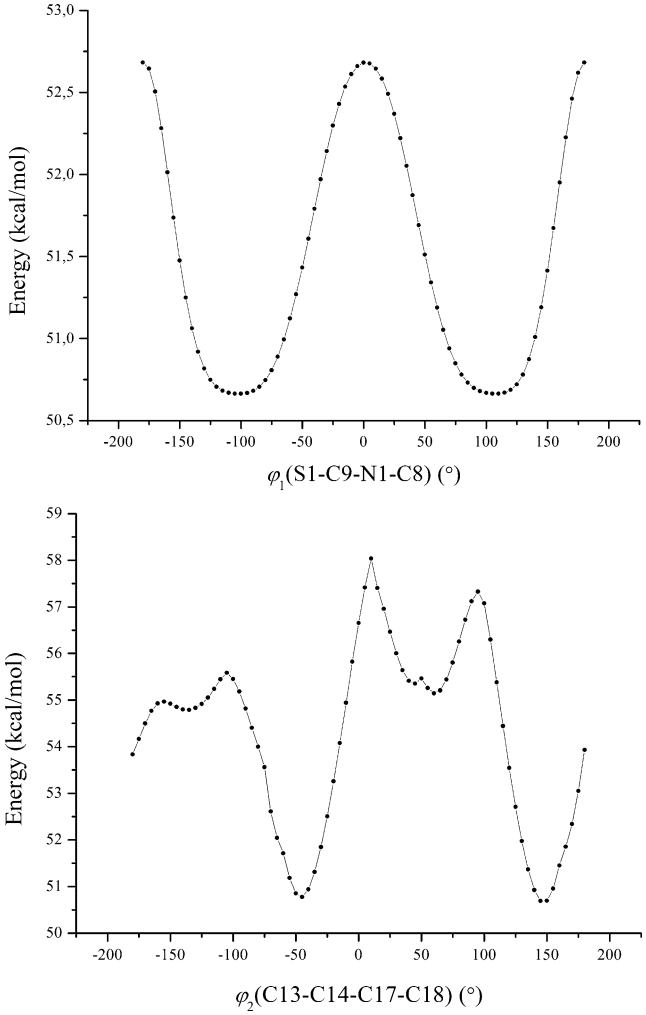

Fig. 5 Molecular energy profiles of the optimized counterpart of the title compound against the selected degrees of torsional freedom

of 0.031 a.u. It is also seen that the electrostatic potential of C1 is more negative than that in the vicinity of C2. What happens to the electrostatic potential when an intramolecular interaction is taking place is that the potential of the negative atom becomes less negative and the positive region on the other atom becomes less positive [41]. So Fig. 6 confirms the existence of an intramolecular interaction between atoms S1 and O2.

Frontier molecular orbitals analysis

Figure 7 shows the distributions and energy levels of the HOMO − 1, HOMO, LUMO and LUMO + 1 orbitals computed at the B3LYP/6–31G(d) level for the title compound. Both the highest occupied molecular orbitals (HOMOs) and the lowest-lying unoccupied molecular orbitals (LUMOs) are mainly located at the rings and mostly the π-antibonding type orbitals. The value of the energy separation between the HOMO and LUMO is

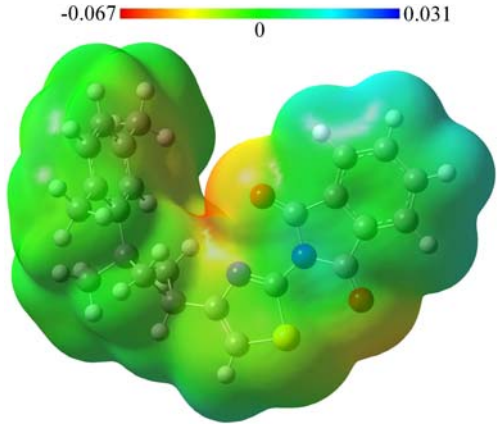

Fig. 6 Molecular electrostatic potential map calculated at B3LYP/6–31G(d) level Frontier molecular orbitals analysis

3.393 eV and this large energy gap indicates that the title structure is quite stable.

Thermodynamic properties

Based on the vibrational analysis at B3LYP/6–31G(d) level and statistical thermodynamics, the standard thermodynamic functions: heat capacity $\left(C^{o}_{p,m}\right)$, entropy $\left(S^{o}_{m}\right)$, and enthalpy $\left(H^{o}_{m}\right)$ were obtained and listed in Table 3. The scale factor for frequencies is 0.9613, which is a typical value for the B3LYP/6–31G(d) level of calculations.

As will be seen from Table 3, the standard heat capacities, entropies and enthalpies increase at any temperature from 100.00 K to 1000.00 K since increasing temperature causes an increase in the intensities of molecular vibration. For the title compound, the correla-

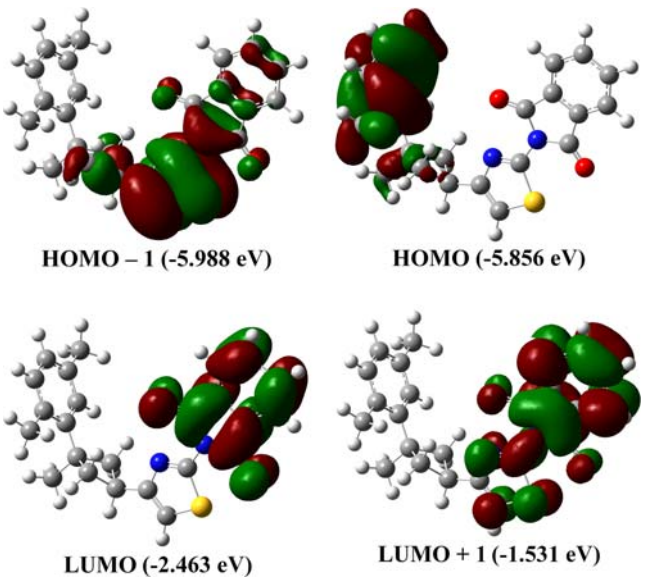

Fig. 7 Molecular orbital surfaces and energy levels given in parentheses for the HOMO −1, HOMO, LUMO and LUMO +1 of the title compound computed at B3LYP/6–31G(d) level

Table 3 Thermodynamic properties of the title compound at different temperatures at B3LYP/6–31G(d) level

T (K)	$C^o_{p,m}(cal.mol^{-1}.K^{-1})$	$S^o_m(cal.mol^{-1}.K^{-1})$	$H^o_m(kcal.mol^{-1})$
100.00	40.937	109.635	2.646
200.00	71.810	148.850	8.479
298.15	103.344	184.177	17.266
300.00	103.935	184.831	17.461
400.00	134.142	219.534	29.597
500.00	159.562	252.738	44.524
600.00	180.091	284.074	61.743
700.00	196.662	313.431	80.808
800.00	210.208	340.870	101.372
900.00	221.428	366.531	123.170
1000.00	230.818	390.570	145.995

tion equations between these thermodynamic properties and temperature T are as follows:

$$C^0_{p,m} = 0.85084 + 0.39848T - 1.69302 \times 10^{-4}T^2 \quad (R^2 = 0.99943) \tag{1}$$

$$S^0_m = 69.58544 + 0.41177\,T - 9.0815 \times 10^{-5}T^2 \quad (R^2 = 0.99999) \tag{2}$$

$$H^0_m = -4.74308 + 0.04585T + 1.06478 \times 10^{-4}T^2 \quad (R^2 = 0.99932) \tag{3}$$

These equations will be helpful for the further studies of the title compound.

IR spectroscopy

FT-IR spectra are obtained in KBr discs using a Mattson 1000 FT-IR spectrometer, and shown in Fig. 8. Based on optimized geometries, the vibrational frequencies have been performed by the same methods and basis sets as. The vibrational bands assignments have been made by using Gauss-View molecular visualization program [26]. Frequency calculations at the same levels of theory revealed no imaginary frequencies, indicating that an optimal geometry at these levels of approximation was found for the title compound.

Our calculations of the title compound are compared to the experimental results. Theoretical and experimental results of the title compound are shown in Table 4. The experimental C=O stretching modes were observed at 1787 and 1725 cm^{-1}, that have been calculated at 1856–1804, 1833–1777, 1837–1768 cm^{-1} for HF levels, 1796–1739, 1771–1725, 1750–1697 cm^{-1} for B3LYP levels. The two bands at 1606 and 1522 cm^{-1}, which can be attributed to the C=N stretching vibrations, have been calculated at 1594–1523, 1579–1506, 1652–1612 cm^{-1} for HF levels, 1522–1493, 1507–1460, 1561–1542 cm^{-1} for B3LYP levels.

Comparing calculational and the experimental data, we studied the relativity between the calculations and the experiments, and obtained linear function formulas are $y = 1.001936x - 4.89124 (R^2 = 0.99882)$ for HF/6–31G(d), $y = 0.99046x + 7.38865 (R^2 = 0.99888)$ for HF/6–31 + G(d,p), $y = 1.05746x - 28.95311 (R^2 = 0.99881)$ for HF/

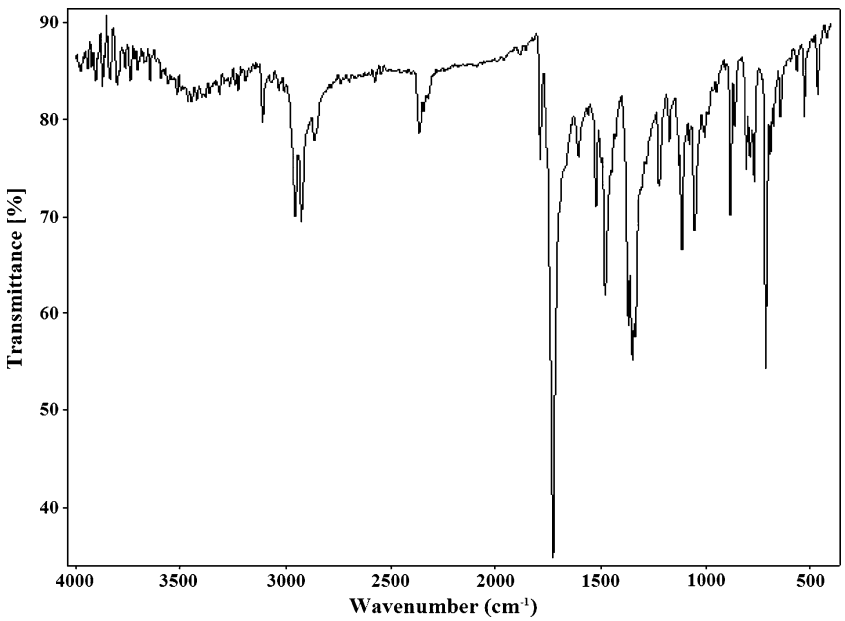

Fig. 8 FT-IR spectrum of the title compound

Table 4 Comparison of the observed and calculated vibrational spectra of the title compound

Assignments	Experimental FT-IR (cm^{-1})	Calculated (cm^{-1})					
		HF			B3LYP		
		6–31G(d)	6–31 + G(d,p)	LANL2DZ	6–31G(d)	6–31 + G(d,p)	LANL2DZ
ν C–H	3110	3080	3052	3273	3142	3131	3292
ν_{as} C–H_2	2956	2950	2924	3127	3011	3002	3148
ν_{as} C–H_3	2925	2924	2912	3066	2973	2964	3097
ν_{s} C–H_3	2862	2858	2862	3000	2919	2909	3026
ν_{s} C=O	1787	1856	1833	1837	1796	1771	1750
ν_{as} C=O	1725	1804	1777	1768	1739	1725	1697
ν C=C (aromatic)	1654	1625	1609	1656	1606	1592	1659
ν C=N	1606	1594	1579	1652	1522	1507	1561
ν C=N	1522	1523	1506	1612	1493	1460	1542
α CH_3	1477	1471	1448	1541	1471	1446	1512
ν C–N	1368	1374	1364	1418	1313	1313	1357
γ CH	1349	1355	1341	1425	1342	1329	1383
ν C–N	1336	1315	1303	1364	1299	1285	1324
γ CH (aromatic)	1222	1182	1262	1230	1266	1259	1237
γ CH (aromatic)	1174	1158	1174	1181	1192	1180	1201
γ CH	1127	1139	1129	1204	1126	1126	1182
ν C–N	1113	1118	1110	1155	1121	1066	1074
ν C–S	1077	1084	1076	1113	1107	1061	1068
ν S–CH	861	830	825	851	825	828	838
ω CH (aromatic)	807	801	813	805	796	790	831
ω CH	790	786	774	867	721	727	803
β_{ring}	692	683	698	709	700	694	694
β_{ring}	677	662	679	697	677	675	676
β_{ring}	644	634	658	667	654	629	650
β_{ring}	566	567	564	556	568	566	585
ω CH (aromatic)	466	464	461	486	461	457	470

ν, stretching; β, bending; α, scissoring; γ , rocking; ω, wagging; δ, twisting; s, symmetric; as, asymmetric

LANL2DZ, $y = 1.02114x - 32.03927$ $(R^2 = 0.99814)$ for B3LYP/6–31G(d), $y = 1.01999x - 43.78966$ $(R^2 = 0.99806)$ for B3LYP/6–31 + G(d,p), and $y = 1.06977x - 69.6133$ $(R^2 = 0.9971)$ for B3LYP/LANL2DZ. According to these results, it is seen that the results of HF/6–31 + G (d,p) method have shown better fit to experimental ones than the others in evaluating vibrational frequencies.

NMR spectroscopy

GIAO ^{13}C and ^{1}H chemical shift calculations have been carried out using the HF and B3LYP methods with 6–31G (d), 6–31 + G(d,p) and LANL2DZ basis sets for the optimized geometry. The results of these calculations are tabulated in Table 5. Since experimental ^{1}H chemical shift values were not available for individual hydrogen, we have presented the average values for CH_2 and CH_3 hydrogen atoms. The singlet observed at 6.86 ppm is assigned to H10 (C10) atoms that have been calculated at 6.25, 7.00, and 7.49 ppm for HF levels, at 6.36, 7.37, and 7.71 ppm for B3LYP levels. The -CH_2- signals of the cyclobutane are observed at 2.62–2.71 ppm. The C-H signals of phenyl adjacent to the cyclobutane are shielded at 6.96, 6.89, and 6.97 ppm. However, the C-H signals belonging to isoindoline group are deshielded at 7.79–7.84 and 7.96–8.00 ppm.

^{13}C-NMR spectra of the thiazol compound show the signals at 165.219 and 111.969 ppm due to C atoms next to sulfur atom. These signals have been calculated as 156.39–113.54, 157.41–115.21, and 174.88–138.55 ppm for HF levels, 150.49–110.04, 154.19–121.18, and 171.48–142.92 ppm for B3LYP levels. The signal at 151.292 ppm is assigned to the C atom next to nitrogen atom of thiazol ring, respectively. While the C atoms of methylene group belonging to the cyclobutane ring are observed at 41.915 ppm,

Table 5 Theoretical and experimental ^{13}C and ^{1}H isotropic chemical shifts (with respect to TMS, all values in ppm) for the title compound

Atom	Experimental (ppm) $CDCl_3$	Calculated chemical shift (ppm)					
		HF			B3LYP		
		6–31G(d)	6–31 + G(d.p)	LANL2DZ	6–31G(d)	6–31 + G(d.p)	LANL2DZ
C1	158.776	157.85	162.74	182.92	160.15	165.94	179.66
C2	135.262	128.96	130.82	136.48	124.38	130.04	133.11
C3	126.701	122.28	123.44	133.19	118.48	121.33	129.84
C4	131.657	130.06	133.21	145.05	128.36	131.48	141.34
C5	131.657	130.05	133.19	145.03	128.78	131.82	141.37
C6	126.701	122.27	123.46	133.19	118.85	120.10	129.70
C7	135.262	128.95	130.81	136.46	125.08	129.53	133.18
C8	158.776	157.89	162.78	182.94	155.94	166.03	179.54
C9	165.219	156.39	157.41	174.88	150.49	154.19	171.48
C10	111.969	113.54	115.21	138.55	110.04	121.18	142.92
C11	151.292	148.93	151.82	164.02	147.01	155.11	163.92
C12	31.570	27.43	27.79	26.71	33.09	35.81	39.23
C13	41.915	34.09	35.13	39.89	41.48	46.46	51.66
C14	40.147	32.72	34.09	36.28	42.17	45.70	51.41
C15	41.915	35.04	36.03	40.69	42.36	44.07	52.34
C16	27.677	24.84	24.92	27.43	27.36	29.62	32.30
C17	149.273	145.16	148.97	159.73	142.62	147.15	154.82
C18	131.475	127.23	130.36	139.52	126.06	131.85	137.89
C19	131.308	127.75	128.74	139.72	124.29	127.46	136.27
C20	126.655	122.33	122.44	132.56	119.26	121.90	130.21
C21	135.444	131.20	134.81	143.95	128.66	133.21	140.23
C22	124.538	123.58	124.59	135.33	120.50	123.43	132.31
C23	19.798	18.21	17.66	20.25	21.18	22.23	27.68
C24	21.278	18.45	18.22	20.53	21.28	21.40	27.40
H3	7.96–8.00 (m)	7.96	8.38	8.96	7.87	8.15	8.56
H4	7.79–7.84 (m)	7.61	8.06	8.66	7.78	8.05	8.57
H5	7.79–7.84 (m)	7.61	8.06	8.67	7.78	8.08	8.54
H6	7.96–8.00 (m)	7.97	8.39	8.98	7.84	8.21	8.57
H10	6.86 (s)	6.25	7.00	7.49	6.36	7.37	7.71
H12	3.91 (q, *j*=8.4 Hz)	5.83	3.09	3.32	3.51	3.61	3.76
H13	2.62–2.71 (m)	2.23*	2.20*	2.24*	2.77*	2.53*	2.81*
H15	2.62–2.71 (m)	2.28*	2.25*	2.32*	2.64*	2.78*	2.90*
H16	1.56 (s)	1.05*	1.05*	1.18*	1.45*	1.35*	1.63*
H19	6.96 (s)	6.79	7.13	7.69	6.96	7.23	7.62
H20	6.89 (d, *j*=7.7 Hz)	6.65	6.95	7.54	6.93	7.16	7.59
H22	6.97 (d, *j*=7.7 Hz)	6.75	7.01	7.48	6.75	7.01	7.55
H23	2.24 (s)	1.72*	1.82*	1.80*	2.09*	2.19*	2.17*
H24	2.30 (s)	1.81*	1.93*	1.89*	2.10*	2.17*	2.19*

* Average

methine C atom appeared at 31.570 ppm. The signal at 40.147 ppm is related to last the C atom of cyclobutan ring.

Comparing calculational and the experimental data, we studied the relativity between the calculations and the experiments, and obtained linear function formulas are $y = 0.98103x - 1.13878$ $(R^2 = 0.99843)$ for HF/6–31G(d), $y = 0.9998x - 1.27407$ $(R^2 = 0.99802)$ for HF/6–31 + G(d,p), $y = 1.09088x - 1.48635$ $(R^2 = 0.99434)$ for HF/LANL2DZ, $y = 0.95219x + 0.67336$ $(R^2 = 0.99801)$ for B3LYP/6–31G(d), $y = 0.98576x + 1.03965$ $(R^2 = 0.99605)$

for B3LYP/6–31 + G(d,p), and $y = 1.05151x + 1.93612$ $(R^2 = 0.99136)$ for B3LYP/LANL2DZ. According to these results, it is seen that the results of HF/6–31G(d) method have shown a better fit to experimental ones than the others in evaluating ^1H and ^{13}C chemical shifts.

Conclusions

In this study, we have synthesized a novel thiazol compound, $C_{24}H_{22}N_2O_2S$, and characterized by spectroscopic (FT-IR and NMR) and structural (XRD) techniques. As a result, the X-ray structure is slightly different from its optimized counterparts, and the crystal structure is stabilized by C—H···S and C—H···O type hydrogen bonds and π—π (face-to-face) interactions. Crystal packing of the title compound is dominated only by intermolecular interactions formed during preparation or crystallization. These hydrogen bonds supply the leading contribution to the stability and to the order of the crystal structure, and are presumably responsible for the discrepancies between the X-ray and optimized structures of the title compound. To test the HF and DFT level of theory with different basis sets reported, computed and experimental geometric parameters, vibrational frequencies and chemical shifts of the title compound have been compared. To fit the theoretical frequency results with the experimental ones for HF and B3LYP levels, we have multiplied the data. For the geometric parameters, the results of B3LYP method has shown a better fit to experimental ones than HF in evaluating geometrical parameters. It was noted here that the experimental results belong to solid phase and theoretical calculations belong to gaseous phase. In the solid state, the existence of the crystal field along with the intermolecular interactions have connected the molecules together, which result in the differences of bond parameters between the calculated and experimental values. However, the HF method seems to be more appropriate than the B3LYP method for the calculation of vibrational frequencies and chemical shifts.

Acknowledgments This study was supported financially by the Research Centre of Ondokuz Mayıs University (Project No: F-461).

References

1. Barone R, Chanon M, Gallo R (1979) In: Metzger JV (ed) Aminothiazoles and their derivatives: The chemistry of heterocyclic compounds- Interscience Publishers, Wiley, New York, vol 34, part 2, pp 9–366
2. Crews P, Kakou Y, Quinoa E (1988) J Am Chem Soc 110 (13):4365–4368
3. Shinagawa H, Yamaga H, Houchigai H, Sumita Y, Sunagawa M (1997) Bioorg Med Chem 5(3):601–621
4. Shivarama Holla B, Malini KV, Sooryanarayana Rao B, Sarojini BK, Suchetha Kumari N (2003) Eur J Med Chem 38(3):313–318
5. Nam G, Lee JC, Chi DY, Kim J-H (1990) B Korean Chem Soc 11 (5):383–386
6. Ibatullin UG, Petrushina TF, Leitis LY, Minibaev IZ, Logvin BO (1993) Khim Geterotsikl Soedin 5:715–718
7. Roger E, Pierre CJ, Pualette V, Gerard G, Chepat JP, Robert G (1977) Eur J Med Chem Chem Ther 12:501–509
8. Golub AG, Yakovenko OY, Prykhod'ko AO, Lukashov SS, Bdzhola VG, Yannoluk SM (2007) Biochim Biophys Acta 1784 (1):143–149
9. Casanovas J, Namba AM, Leon S, Aquino GLB, da Silva GVJ, Aleman C (2001) J Org Chem 66(11):3775–3782
10. Sebag AB, Forsyth DA, Plante MA (2001) J Org Chem 66 (24):7967–7973
11. Forsyth DA, Sebag AB (1997) J Am Chem Soc 119(40):9483–9494
12. Helgaker T, Jaszunski M, Ruud K (1999) Chem Rev 99(1):293–352
13. Ditchfield R (1972) J Chem Phys 56(11):5688–5691
14. Wolinski K, Hinton JF, Pulay P (1990) J Am Chem Soc 112 (23):8251–8260
15. Cheeseman JR, Trucks GW, Keith TA, Frisch MJ (1996) J Chem Phys 104(14):5497–5509
16. Cimino P, Gomez-Paloma L, Duca D, Riccio R, Bifulco G (2004) Magn Reson Chem 42:26–33
17. Friesner RA, Murphy RB, Beachy MD, Ringnalda MN, Pollard WT, Dunietz BD, Cao Y (1999) J Phys Chem A 103(13):1913–1928
18. Rulìsek L, Havlas Z (2003) Int J Quantum Chem 91(3):504–510
19. Ziegler T (1997) Density-functional methods in chemistry and material science. Wiley, New York
20. Rauhut G, Puyear S, Wolinski K, Pulay P (1996) J Phys Chem 100(15):6310–6316
21. Ditchfield R, Hehre WJ, Pople JA (1971) J Chem Phys 54 (2):724–728
22. Frisch MJ, Pople JA, Binkley JS (1984) J Chem Phys 80:3265–3269
23. Hay PJ, Wadt WR (1985) J Chem Phys 82:270–283
24. Wadt WR, Hay PJ (1985) J Chem Phys 82:284–298
25. Hay PJ, Wadt WR (1985) J Chem Phys 82:299–310
26. Dennington II R, Keith T, Millam J (2007) GaussView, Version 4.1.2. Semichem Inc., Shawnee Mission, KS
27. Frisch MJ, Trucks GW, Schlegel HB, Scuseria GE, Robb MA, Cheeseman JR, Montgomery Jr JA, Vreven T, Kudin KN, Burant JC, Millam JM, Iyengar SS, Tomasi J, Barone V, Mennucci B, Cossi M, Scalmani G, Rega N, Petersson GA, Nakatsuji H, Hada M, Ehara M, Toyota K, Fukuda R, Hasegawa J, Ishida M, Nakajima T, Honda Y, Kitao O, Nakai H, Klene M, Li X, Knox JE, Hratchian HP, Cross JB, Bakken V, Adamo C, Jaramillo J, Gomperts R, Stratmann RE, Yazyev O, Austin AJ, Cammi R, Pomelli C, Ochterski JW, Ayala PY, Morokuma K, Voth GA, Salvador P, Dannenberg JJ, Zakrzewski VG, Dapprich S, Daniels AD, Strain MC, Farkas O, Malick DK, Rabuck AD, Raghavachari K, Foresman JB, Ortiz JV, Cui Q, Baboul AG, Clifford S, Cioslowski J, Stefanov BB, Liu G, Liashenko A, Piskorz P, Komaromi I, Martin RL, Fox DJ, Keith T, Al-Laham MA, Peng CY, Nanayakkara A, Challacombe M, Gill PMW, Johnson B, Chen W, Wong MW, Gonzalez C, Pople JA (2004) Gaussian 03, Revision E.01. Gaussian Inc, Wallingford, CT
28. Farrugia LJ (1997) J Appl Crystallogr 30:565

29. Swenson DC, Yamamoto M, Burton DJ (1997) Acta Crystallogr C53:1445–1447
30. Çukurovalı A, Özdemir N, Yılmaz İ, Dinçer M (2005) Acta Crystallogr E61:o1754–o1756
31. Dinçer M, Özdemir N, Yılmaz İ, Çukurovalı A, Büyükgüngör O (2004) Acta Crystallogr C60:o674–o676
32. Allen FH (1984) Acta Cryst B40:64–72
33. Glidewell C, Low JN, Skakle JMS, Wardel JL (2004) Acta Crystallogr C60:o15–o18
34. Bondi A (1964) J Phys Chem 68(3):441–451
35. Clark T, Hennemann M, Murray JS, Politzer P (2007) J Mol Model 13(2):291–296
36. Murray JS, Lane P, Politzer P (2008) Int J Quant Chem 108 (15):2770–2781
37. Politzer P, Murray JS, Concha MC (2008) J Mol Model 14(8):659–665
38. Scrocco E, Tomasi J (1978) Adv Quantum Chem 11:115–121
39. Luque FJ, Lopez JM, Orozco M (2000) Theor Chem Acc 103:343–345
40. Okulik N, Jubert AH (2005) Internet Electron J Mol Des 4:17–30
41. Murray JS, Peralta-Inga Z, Politzer P (1999) Int J Quant Chem 75 (3):267–273